Experimental and modeling study of the thermal decomposition of methyl decanoate

Olivier Herbinet, Pierre Alexandre Glaude, Valérie Warth, Frédérique Battin-Leclerc

Experimental and modeling study of the thermal decomposition of methyl decanoate

Olivier Herbinet[a,*], Pierre-Alexandre Glaude[a], Valérie Warth[a] and Frédérique Battin-Leclerc[a]

[a] Laboratoire Réactions et Génie des Procédés, Nancy Université, CNRS UPR 3349, BP 20451, 1 rue Grandville, 54001 Nancy, France

Abstract

The experimental study of the thermal decomposition of methyl decanoate was performed in a jet-stirred reactor at temperatures ranging from 773 to 1123 K, at residence times between 1 and 4 s, at a pressure of 800 Torr (106.6 kPa) and at high dilution in helium (fuel inlet mole fraction of 0.0218). Species leaving the reactor were analyzed by gas chromatography. Main reaction products were hydrogen, carbon oxides, small hydrocarbons from C_1 to C_3, large 1-olefins from 1-butene to 1-nonene, and unsaturated esters with one double bond at the end of the alkyl chain from methyl-2-propenoate to methyl-8-nonenoate. At the highest temperatures, the formation of polyunsaturated species was observed: 1,3-butadiene, 1,3-cyclopentadiene, benzene, toluene, indene, and naphthalene. These results were compared with previous ones about the pyrolysis of n-dodecane, an n-alkane of similar size. The reactivity of both molecules was found to be very close. The alkane produces more olefins while the ester yields unsaturated oxygenated compounds.

A detailed kinetic model for the thermal decomposition of methyl decanoate has been generated using the version of software EXGAS which was updated to take into account the specific chemistry involved in the oxidation of methyl esters. This model contains 324 species and 3231 reactions. It provided a very good prediction of the experimental data obtained in jet-stirred reactor. The formation of the major products was analyzed. The kinetic analysis showed that the retro-ene reactions of intermediate unsaturated methyl esters are of importance in low reactivity systems.

Keywords: Methyl decanoate; Biodiesel; Jet-stirred reactor; Thermal decomposition; Pyrolysis; Kinetic modeling

*Corresponding author: Olivier Herbinet
Laboratoire Réactions et Génie des Procédés, Nancy Université, CNRS UPR 3349, BP 20451, 1 rue Grandville, 54000 Nancy, France.
Tel : +33 3 83 17 53 60 ; Fax : +33 3 83 37 81 20
E-mail : olivier.herbinet@ensic.inpl-nancy.fr

1. Introduction

Fuel thermal decomposition reactions are of importance in kinetic studies as the interpretation of experimental phenomena is much simpler than in the case of oxidation reactions for the analysis of the primary reaction pathways of a reactant. Furthermore, the sensitive reactions are not quite the same due to the differences in experimental conditions (e.g., no oxygen molecule, higher temperatures in pyrolysis studies). These conditions are of importance in some practical cases such as diesel engines. The first reactions of diesel fuels in the combustion chamber are close to a pyrolysis leading to a high amount of unsaturated products and soot that are later oxidized in the flame front. Thus thermal decomposition and oxidation studies are complementary and both are needed to perform the validation of detailed kinetic models [1].

Amongst new transportation fuels, the interest in biodiesel is increasing because of their use along with conventional diesel fuels in internal combustion engines [2], [3], [4], [5] and [6]. Biodiesel fuels are composed of methyl esters deriving from the trans-esterification of vegetable oils and animal fats. These esters are made of an alkyl chain attached to an ester group, the main differences being the number of carbon atoms and the number of double bonds in the alkyl chain. As an example, palm, rapeseed and soybean biodiesels are mainly composed of C_{17} and C_{19} methyl esters: methyl palmitate ($C_{17}H_{34}O_2$), methyl stearate ($C_{19}H_{38}O_2$), methyl oleate ($C_{19}H_{36}O_2$), methyl linoleate ($C_{19}H_{34}O_2$) and methyl linolenate ($C_{19}H_{32}O_2$). Methyl palmitate and methyl stearate have no Cdouble bond; length as m-dashC double bond whereas methyl oleate, methyl linoleate and methyl linolenate have one, two and three Cdouble bond; length as m-dashC double bonds, respectively [7]. The oxidation of large methyl esters has been the subject of numerous experimental and modeling studies during the last years [7], [8], [9], [10], [11], [12], [13] and [14], but the thermal decomposition of this type of molecules was very little investigated in the past and there is very little data that can be used for the validation of detailed kinetic models.

Hurd and Blunck [15] performed a study of the pyrolysis of seven esters (ethyl, phenyl, i-propyl, i-butyl and t-butyl acetates and methyl and ethyl phenyl-acetates) in sealed tubes (temperatures between 633 and 923 K). The nature of the reaction products (which were analyzed by titration) depends on the initial reactant. In the case of ethyl acetate, reaction products were hydrogen, carbon oxides, methane, ethylene, acetic acid, formaldehyde, acetaldehyde and acetic anhydride. The main result of this study is that esters mainly decompose into organic acid and olefin if there is an H-atom in the β position in the alkyl portion of the ester. Arnold et al. [16] studied the pyrolysis of cis and trans-2-methylcyclohexyl acetates in sealed tubes at 768 K. They also observed the formation of olefins: 1-methyl and 3-methyl-cyclohexene. These authors [15] and [16] proposed different possible mechanisms accounting for the formation of organic acids and olefins, one of them being a concerted elimination through a six membered ring transition state. Blades [17] studied the thermal decomposition of ethyl formate, isopropyl formate, ethyl acetate, and isopropyl acetate in a continuous flow reactor using toluene as carrier gas. Toluene was used as radical scavenger in order to favor molecular reactions. This study confirmed that the mechanism responsible for the formation

of organic acids and olefins is a purely intramolecular decomposition reaction and kinetic parameters were derived from experimental results.

More recently, Archambault and Billaud [18] studied the pyrolysis of rapeseed oil methyl esters (enriched in methyl oletate – 82.1 wt.%) in a tubular flow reactor over the range of temperatures 773–973 K and residence times 0.6–1.2 s. Species at the outlet of the reactor were analyzed by gas chromatography. The conversion of fuel was measured as a function of the temperature. Reaction products were hydrogen, methane, carbon oxides, linear alkanes and olefins form C_2 to C_{18}, aromatics (benzene and toluene), C_3 to C_{16} unsaturated methyl esters, saturated methyl esters (methyl acetate and methyl propanoate), coke and some other minor products (diolefins, polyunsaturated esters). Unfortunately, only the evolution of the selectivity of groups of species was given in this work. In the same area, Seames et al. [19] studied the pyrolysis of canola and soybean methyl esters in a batch reactor at temperatures around 713 K. They observed the formation of the same classes of products as Archambault and Billaud [18] but individual amounts of each reaction products were not given.

Farooq et al. [20] performed an experimental and computational study of the thermal decomposition of three small methyl esters (methyl acetate, methyl propionate and methyl butanoate) in a shock tube over the range of temperatures 1260–1653 K, pressures of 1.4–1.7 atm and reactant concentrations of 2–3% (dilution in argon). Measurements of CO2 time-histories were carried out. They showed that the formation of CO_2 was very little dependent on the size of the alkyl chain and that the three detailed kinetic models from the literature [21], [22] and [23] used for the computation tended to underestimate CO_2 yields. The largest underestimation was obtained with the model from Metcalfe et al. [22], the smallest one with the model of Gaïl et al. [23], with the prediction by the model of Fisher et al. [21] lying in between. An improved model, based on the work of Fisher et al. [21] and the reaction rate calculations from Huynh and Violi [24] provided the best prediction except at the highest temperatures.

This paper presents new detailed experimental results of the thermal decomposition of methyl decanoate (Fig. 1) in a jet-stirred reactor. Methyl decanoate ($C_{11}H_{22}O_2$) was chosen because it has been proposed as a possible surrogate for large species found in biodiesel [9] and because a study of the oxidation of this compound was already performed in a jet-stirred reactor [12]. These new results were compared with previous ones obtained for n-dodecane [25], an n-alkane of similar size, in order to highlight the similarities and the differences between the two types of molecules. A detailed kinetic model for the thermal decomposition of methyl decanoate was generated using the software EXGAS [26], [27] and [28] which was recently used to simulate the oxidation of saturated methyl esters [12]. Computed and experimental data were then compared showing a good agreement.

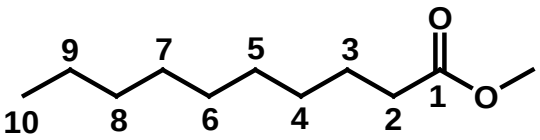

Fig. 1. Structure of methyl decanoate ($C_{11}H_{22}O_2$).

2. Experimental method

The experimental study of the thermal decomposition of methyl decanoate was performed in a jet-stirred reactor operated at constant temperature and pressure. The experimental apparatus has already been described in previous papers [8] and [25]. This type of reactor was already used for numerous pyrolysis and oxidation gas phase studies [7], [8], [9] and [25]. Its main advantage is that it can be easily modeled as a 0 dimensional ideal perfectly stirred reactor as the temperature and the composition in the reactor are homogenous. Figure 2 displays a scheme of the experimental apparatus used in this study. The main features of the experimental and analytical methods are described below.

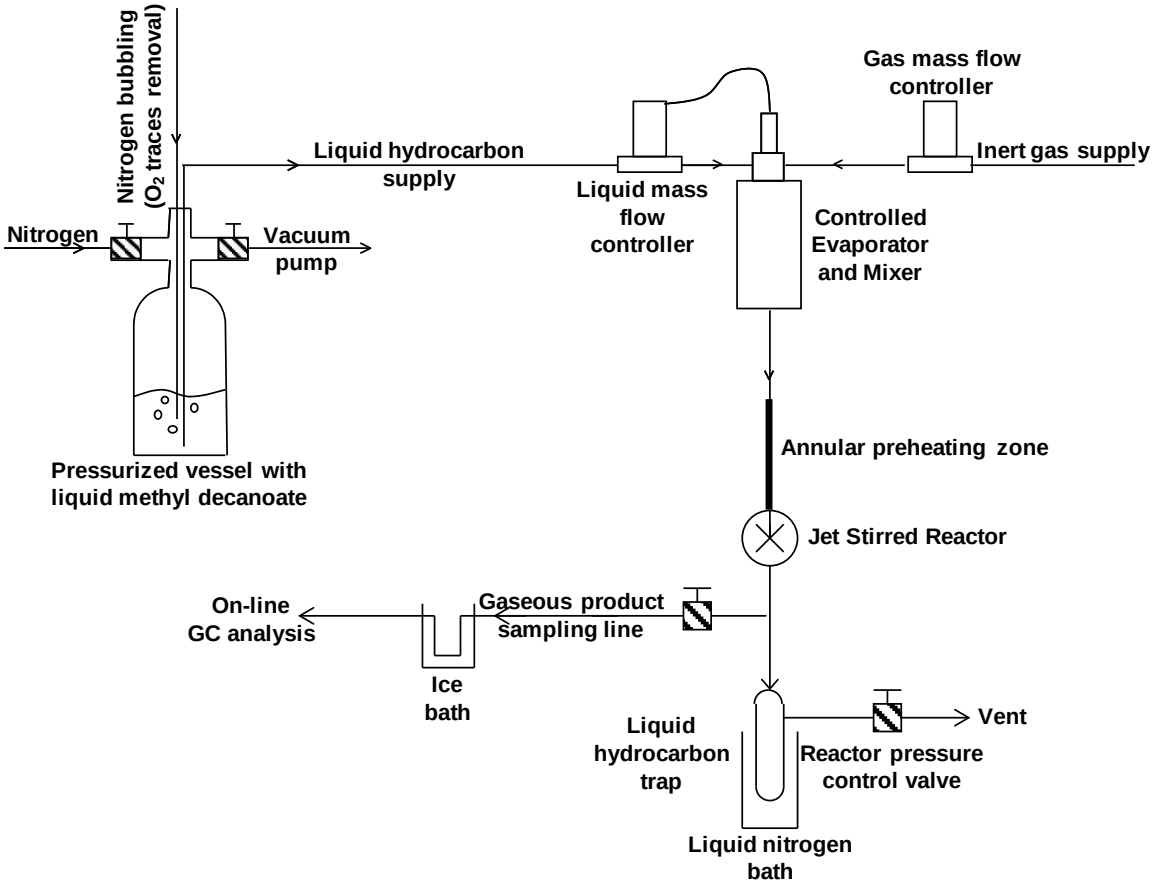

Fig. 2. Scheme of the experimental apparatus used in this study.

The jet-stirred reactor is made of fused silica to minimize catalytic reactions at the wall. It consists of an annular preheater (for a progressive heating of the reacting mixture up to the reaction temperature in a very short time – heating rates of 106 K s^{-1} can be reached according to Houzelot and Villermaux [29] and [30]; this is very important to avoid strong temperature gradients in the reactor) and of a sphere in which the reaction takes place (with an injection cross located at its center). The reactor (volume of 90 cm3) and the injection cross were designed in order to obtain four turbulent jets providing a good mixing of the gas phase (thus concentrations at the outlet and inside the reactor are the same) [31]. The heating of the preheater and of the reactor is achieved by the mean of Thermocoax resistances rolled around the different parts and controlled by Eurotherm 3216 controllers and type K thermocouples (temperature precision better than 1%). The heating of the preheater is divided in two zones, the first one being heated at a temperature 150 K lower than the reaction temperature and the second one being heated at the same temperature as the reactor. The reaction temperature was measured by another type K thermocouple located in the intra annular part of the preheater with its extremity at the level of the injection cross in the center of the reactor.

The feed of liquid methyl decanoate (provided by SAFC, purity: 99+) was controlled thanks a liquid mass flow controller provided by Bronkhorst. This device was associated to an evaporator (also provided by Bronkhorst) in which methyl decanoate was mixed with the carrier gas (helium IC, provided by Messer) and heated to 473 K. Helium flow rate was controlled by a Tylan gas mass flow controller. Helium was used to avoid the condensation of the carrier gas during the sampling at liquid nitrogen temperature at the outlet of the reactor. The pressure in the reactor was maintained constant at 800 Torr (106.6 kPa) using a valve located downstream of the reactor (a pressure of 800 Torr was required because of the pressure drops in the sampling valves of online gas chromatographs).

Reaction products and unconverted reactant exiting the reactor were analyzed by the mean of several gas chromatographs. The analysis was performed in two steps as light and heavy species could not be analyzed at the same time. Heavy species (including at least five heavy atoms such as carbon and oxygen ones) were condensed in a trap connected to the reactor outlet and maintained at liquid nitrogen temperature. After a known period of time (typically five minutes), the trap was disconnected. Once the trap warmed up to the ambient temperature, an internal standard (n-octane) and a solvent (acetone) were added in it. The content of the trap was then injected in an Agilent 6850 gas chromatograph fitted with a HP-1 capillary column and a flame ionization detector (FID). Light species (including less than six heavy atoms) were analyzed online using two gas chromatographs. Both were fitted with a sampling valve (loop volume of 250 µL) for the injection of the gaseous mixture from the reactor. The first gas chromatograph (Agilent 6850) was fitted with a Plot-Q capillary column (providing a good separation for light hydrocarbons from methane to 1-pentene and oxygenated compounds such as acetaldehyde) and a FID. The second gas chromatograph (Agilent 7890) was fitted with a Carbosphere packed column (providing a good separation for very light species such as methane, C_2 hydrocarbons, carbon oxides and hydrogen), a thermal conductivity detector (TCD) and a FID associated to a methanizer. The use of a methanizer fitted with the FID provides a better sensitivity for the quantification of oxygenated species such as

carbon oxides which are usually quantified by TCD: carbon oxides were detected at concentrations less than 10 ppm in the present study. As hydrogen was the only product quantified using TCD (carbon oxides were quantified using FID), it was possible to use argon as a carrier and reference gas to enhance the sensitivity (the limit of detection of hydrogen was 90 ppm). For other hydrocarbons and oxygenated species (mainly unsaturated methyl esters) the limit of detection was between 1 and 10 ppm according to the size of the molecule.

3. Experimental results

The thermal decomposition of methyl decanoate was studied at a pressure of 106.6 kPa and an inlet fuel mole fraction of 0.0218. A first set of experiments was performed at a constant residence time of 1 s and at temperatures ranging from 773 to 1123 K. Two other sets of experiments were performed at 873 and 973 K by varying the residence time from 1 to 4 s.

Reaction products observed during this study can be classified in the following way:

- Small oxygenated compounds: carbon oxides, acetaldehyde.
- Hydrogen and small hydrocarbons: methane, acetylene, ethane, propyne, allene, propane, 1,3-butadiene and 1,3-cyclopentadiene.
- Olefins from ethylene to 1-nonene.
- Unsaturated esters with one double bond at the end of the alkyl chain from methyl-2-propenoate ($C_4H_6O_2$) to methyl-8-nonenoate ($C_{10}H_{18}O_2$). The structures of these species are given in Table 1.
- Aromatic and poly-aromatic compounds: benzene, toluene, styrene, indene and naphthalene.

Table 1. List of unsaturated esters observed in this study.

Structure	Name	Global formula	Molar weight ($g.mol^{-1}$)
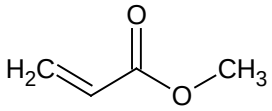	Methyl-2-propenoate	$C_4H_6O_2$	86
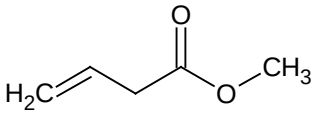	Methyl-3-butenoate	$C_5H_8O_2$	100
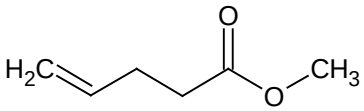	Methyl-4-pentenoate	$C_6H_{10}O_2$	114
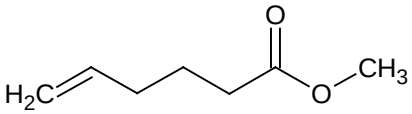	Methyl-5-hexenoate	$C_7H_{12}O_2$	128
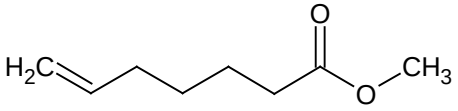	Methyl-6-heptenoate	$C_8H_{14}O_2$	142
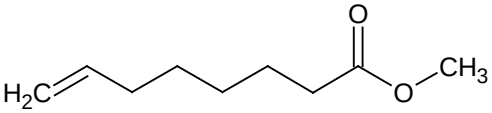	Methyl-7-octenoate	$C_9H_{16}O_2$	156
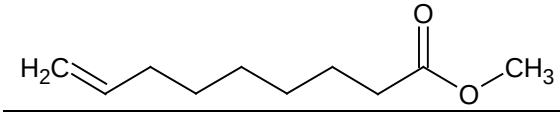	Methyl-8-nonenoate	$C_{10}H_{18}O_2$	170

Figure 3 displays the evolution of the conversion of the fuel with the temperature at a constant residence time of 1 s (Fig. 3a) and with the residence time at 873 and 973 K (Fig. 3b). Figure 3a shows that the consumption of the fuel becomes significant above 873 K. [Fig. 4], [Fig. 5], [Fig. 6] and [Fig. 7] display the evolution of the mole fractions of reaction products with the temperature. An excel spreadsheet with mole fractions of the species detected in this study is available in Supplementary material. The formation of some reaction products (such as carbon oxides, olefins and unsaturated esters, with mole fractions between 1 and 10 ppm) is already observed at 773 K, meaning that the decomposition of the fuel is already occurring at the lowest temperature studied in this work. Mole fraction profiles of most reaction products (1-pentene and larger olefins, methyl-4-pentenoate and larger unsaturated esters) exhibit a maximum at about 950 K. Mole fraction profiles of propene, 1-butene, methyl-2-propenoate and methyl-3-butenoate also exhibit a maximum but it is located at higher temperature. These latter species are not only primary products but are partly formed during the decomposition of larger olefins and unsaturated esters. Profiles of small alkanes (ethane, propane) and of aromatic compounds such as benzene and toluene display also a maximum. Mole fractions of small unsaturated hydrocarbons (acetylene, allene, propyne) and larger aromatics (styrene, indene, naphthalene) are increasing in the whole temperature range of this study. Carbon oxides, which come from the decomposition of the ester group, have mole fractions increasing with the temperature. Mole fractions of hydrogen increase in a monotonous way with the temperature as this species comes from the dehydrogenation of hydrocarbons.

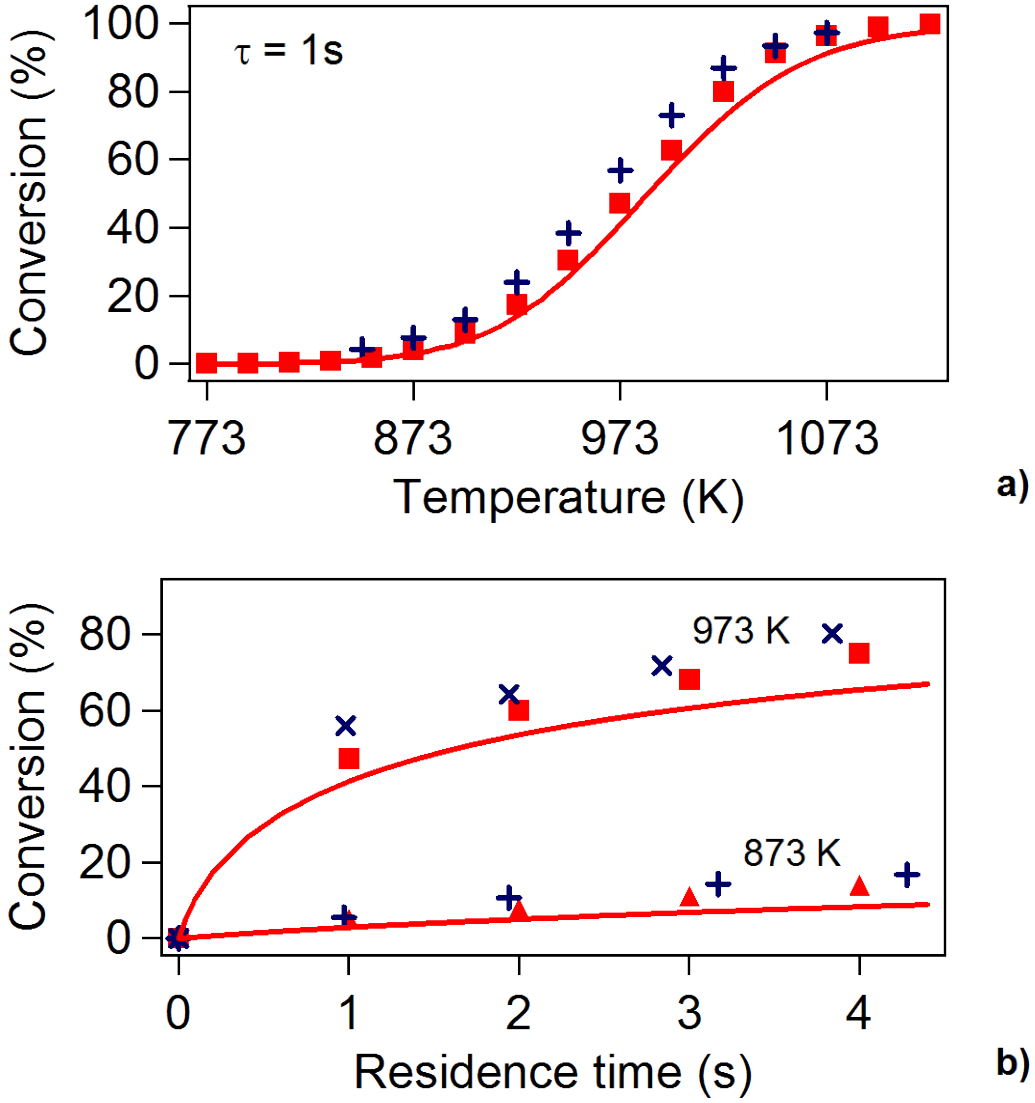

Fig. 3. Evolution of the conversion of the reactant with (a) the temperature and (b) the residence time (■ and up triangle, filled: methyl decanoate experiments; × and +: n-dodecane experiments [25]; line: methyl decanoate simulations). Inlet mole fractions of n-dodecane and methyl decanoate are 0.02 and 0.0218, respectively.

The experimental results of the thermal decomposition of methyl decanoate ($C_{11}H_{22}O_2$) were compared with a set of already published data about the pyrolysis of n-dodecane ($C_{12}H_{26}$) under similar conditions [25] in order to highlight the differences between large n-alkanes and methyl esters. The carbon content in both sets of experiments is almost the same as the inlet fuel mole fractions were 0.02 for n-dodecane and 0.0218 for methyl decanoate. It can be seen in Fig. 3 that n-dodecane and methyl decanoate have very close reactivities, n-dodecane being slightly more reactive. As far as reaction products are concerned, the formation of unsaturated methyl esters and oxygenated species was not observed in the n-dodecane study as this hydrocarbon does not contain oxygen atom. The comparison between both sets of experiments showed that the main differences are observed for 1-olefins: mole fractions of these species are lower in the case of methyl decanoate

and the difference tends to disappear for smaller 1-olefins (there is almost no difference for ethylene and propene). This can be explained by the fact that ester-alkyl radicals can decompose either to 1-olefins or to unsaturated esters whereas alkyl radicals only decompose to 1-olefins. The difference tends to disappear for small species which are not only formed from the decomposition of alkyl and ester-alkyl radicals but also from the decomposition of larger 1-olefins and unsaturated esters. Note that mole fractions of 1-octene are similar with both fuels. This is due to the fact that the formation of 1-octene is favored in the case of methyl decanoate by the low energy of the C-C bond in the α position of the ester function. The comparison between the methyl ester and the alkane also shows that there is almost no difference for the smallest species (e.g., hydrogen, methane, ethane, acetylene, allene, propyne). This can be explained by the same reason as for the small olefins. For 1,3-cyclopentadiene and aromatic compounds, some differences are observed. With n-dodecane, mole fractions of 1,3-cyclopentadiene, benzene, indene and naphthalene are slightly larger whereas they are lower for toluene and styrene. There is no obvious reason that explains these slight differences.

4. Modeling

A model for the pyrolysis of methyl decanoate was generated using software EXGAS, which was initially developed for the oxidation of alkanes [26], [27] and [28] and which has been recently updated for the oxidation of saturated esters [12]. Some reactions, which were not included in the model generated using software EXGAS, have been added to account for the decomposition of unsaturated esters (this point is discussed later). This model contains 3231 reactions involving 324 species and is made of three parts:

- A comprehensive primary mechanism (1200 reactions) in which the only reacting molecule is the initial reactant (methyl decanoate) and the free radicals produced. The molecules formed in this part of the model are called primary products. Their fate is considered in the secondary mechanism.
- A lumped secondary mechanism (805 reactions) which contains the reaction of the primary products. Lumping consists in considering that all the species having the same chemical formula and the same functional groups are gathered into one unique species (e.g., all $C_7H_{12}O_2$ unsaturated esters are represented by one species in the model, whatever the position of the C=C double bond). In order to keep the size of the mechanism compatible with simulations, the reactions of lumped species are not any more elementary steps but global reactions which represent some successive elementary reactions, with a rate parameter corresponding to that of the limiting step. Reactions are written in order to promote radicals which already exist in the primary mechanism. Lumping provides a significant decrease of the numbers of species and reactions.
- A comprehensive C_0-C_8 reaction base (1226 reactions) which contains all the reaction of small species having no more than two carbon atoms, unsaturated C_3 and C_4 unsaturated hydrocarbons and first aromatics (benzene, toluene and styrene) [32]. Two reactions of consumption of the radical •C(=O)-O-CH_3, which is specific to esters, were added in the C_0-C_2 reaction base. These reactions have already been described in [12]. The C_3-C_4 reaction base

[32] is an extension of the previous C_0-C_2 reaction base [33]. It was built from a review of the literature. The reactions of the first aromatics come from the oxidation mechanism developed for benzene [34] and toluene [35]. This C_0-C_8 reaction base was successfully tested against experimental data from the study of rich premixed laminar flames doped with 1,3-butadiene [32].

Some pericyclic molecular reactions, which were not originally included in the model, were added in the secondary mechanism to account for the consumption of unsaturated esters. These reactions are called retro-ene and consist in a decomposition into propene and smaller unsaturated esters through a concerted mechanism involving a six membered ring cyclic transition state. These reactions are well known in the case of olefins (Fig. 8). Thermal decomposition studies [25] and [36] showed that they play an important role in the consumption of these large olefins. Retro-ene reactions have been added in the case of unsaturated methyl ester (Fig. 8), with the same rate constant as that used for the alkenes, i.e. $k = 8.0 \times 10^{12} \exp(-56{,}500 \text{ cal mol}^{-1}/RT)\ s{-}1$ as proposed by Richard et al. [37]. The retro-ene reactions involve the transfer of an H-atom in the γ position of the C=C double bond and consequently cannot happen for small unsaturated esters (methyl-4-pentenoate, methyl-3-butenoate and methyl-2-propenoate).

Unimolecular initiations are usually negligible in the secondary mechanism and these reactions were not written except in the case of methyl-4-pentenoate. This species has a particular C-C bond in the β position of the ester group with a relatively low energy. The breaking of this bond, yielding allyl and $\bullet CH_2COOCH_3$ radicals, requires only 70.7 kcal mol^{-1}.

A model, with no specific molecular reactions for the decomposition of methyl-4-pentenoate, methyl-3-butenoate and methyl-2-propenoate, was tested against the set of experimental data obtained in a jet-stirred reactor ([Fig. 3], [Fig. 4], [Fig. 5], [Fig. 6] and [Fig. 7]). It can be seen that the model accounts for the consumption of the reactant and the mole fractions of most reaction products except methyl-4-pentenoate and methyl-3-butenoate which are over-predicted (of about a factor of 2), meaning that a pure radical mechanism is not sufficient to account for the consumption of these particular species.

Thus some quantum calculations were performed in order to find other possible consumption routes for methyl-3-butenoate and methyl-4-pentenoate. Molecular reactions have been investigated in the case of methyl-3-butenoate and methyl-4-pentenoate. The calculations have been performed using Gaussian 03 (Rev. C.02) [38] and the composite CBS-QB3 method [39]. Frequency analysis has made it possible to point out one imaginary frequency for each transition state (TS) and IRC calculations confirmed that the TS connected the reactant to the products. Figure 9 presents the different reaction channels and the energy barriers found in the case of methyl-3-butenoate. The pericyclic reactions involving the lowest energy barrier are the isomerizations to methyl crotonate through a four-centered H-transfer (reactions (1) and (2)). Trans and cis methyl crotonate can be obtained, the

latter involving a slightly higher activation energy. Another four-centered reaction consists in the transfer of a H-atom from the α position of the ester group to the O-atom, yielding an acetal (reaction (3)). The transfer of the H-atoms in α position of the ester group and of the C=C double bond is easy: the C-H bond is particularly weak because of the stabilization induced by these two groups. By analogy with the reaction of the carboxylic acids, reactions of transfer or elimination of the methoxy group (reactions (4) and (6)) have been investigated. The energy barriers found, respectively 77.4 and 84.0 kcal mol^{-1}, prevent these reactions to play any role. The transfer of the methyl group producing CO_2 and 1-butene (reaction (5)) is very exothermic but involves also a high activation energy, showing that a direct production of CO2 through a molecular reaction should be negligible in the reaction of methyl esters. The rate constants of the three reactions with the lowest energy barriers were determined. High-pressure limit unimolecular rate constants were calculated using classical TS theory and the CHEMRATE software [40]. For reactions involving a H-transfer, a transmission coefficient has been calculated in order to take into account the tunneling effect using Eckart potential [41]. The kinetic parameters were obtained from a fitting between 700 and 1300 K, with a modified Arrhenius form. The rate constants are, with activation energy in cal mol^{-1}:

$C_5H_8O_2 \rightarrow$ trans methyl crotonate $\quad k = 1.01 \times 10^7 \, T^{1.74} \exp(-64{,}810 / RT) \, s^{-1}$ (1)

$C_5H_8O_2 \rightarrow$ cis methyl crotonate $\quad k = 1.37 \times 10^7 \, T^{1.68} \exp(-63{,}560 / RT) \, s^{-1}$ (2)

$C_5H_8O_2 \rightarrow CH_2CHCHC(OH)(OCH_3)$ $\quad k = 1.23 \times 10^{-3} \, T^{4.44} \exp(-57{,}490 / RT) \, s^{-1}$ (3)

The product of reaction (3) decomposes easily since the O-CH_3 bond dissociation energy is only 42.8 kcal mol^{-1}. A global decomposition into CO_2, methyl and allyl radicals was considered.

In the case of methyl-4-pentenoate, the four-centered H-transfer are more difficult since the C-H bonds on the alkyl chain are stronger that in methyl-3-butenoate. The only reaction with a low energy barrier is a six-centered isomerization presented in Fig. 10. The rate constant has been computed using transition state theory with calculations at the CBS-QB3 level of theory: $k = 1.26 \times 10^7 \, T^{1.23} \exp(-55{,}800/RT) \, s^{-1}$. The reaction product is very unstable and decomposes easily into allyl radical and $\bullet OCH_2COCH_3$ radical, which is a mesomeric form of $\bullet CH_2COOCH_3$, because of the low C-O bond dissociation energy (34.4 kcal mol^{-1}).

Despite this effort, the inclusion of these new reactions has very little effect on the mole fractions of methyl-4-pentenoate and methyl-3-butenoate, which are still over-predicted. A-factors must be increased by more than a factor of 100 to observe a significant effect, meaning that there are likely other pathways for the consumption of these unsaturated esters. Note that the formation of methyl crotonate was not observed in the experiments, confirming the little importance of reaction (1) and (2) in the simulations due to their high activation energies.

Thermodynamic properties of molecules and radicals involved in the model were automatically calculated using THERGAS software [42], based on the group and bond additivity methods proposed by Benson [43]. These data are stored as 14 polynomial coefficients, according to the CHEMKIN II formalism [44]. Bond dissociation energies of C-H, C-O, and -C bonds close to the ester function were updated from the values recently proposed by El-Nahas et al. [45]. These changes were described in detail in [12] and [46].

5. Discussion

The model presented in the previous section was used to compute the mole fractions of the reactant and of reaction products. The conversion of the reactant is fairly well reproduced (Fig. 3). The agreement is also satisfactory for most reaction products: hydrogen, methane, ethylene and larger olefins ([Fig. 4] and [Fig. 5]), and unsaturated esters in Fig. 6 (except methyl-3-butenoate and methyl-4-pentenoate, for which some decomposition pathways are likely missing as discussed in the model section). The general good agreement, which is observed for olefins and unsaturated esters, means that the rules used for the generation of the primary mechanism well account for the formation and consumption pathways of these species. The main discrepancies are observed for species with several unsaturations. Allene and propyne profiles are fairly well reproduced by the model (Fig. 4), whereas mole fractions of 1,3-butadiene, 1,3-cyclopentadiene, benzene and toluene are slightly under-estimated (Fig. 7). Mole fractions of styrene are slightly over-estimated at the higher temperatures. Styrene is the largest aromatic compound considered in the model and no consumption reaction has been included.

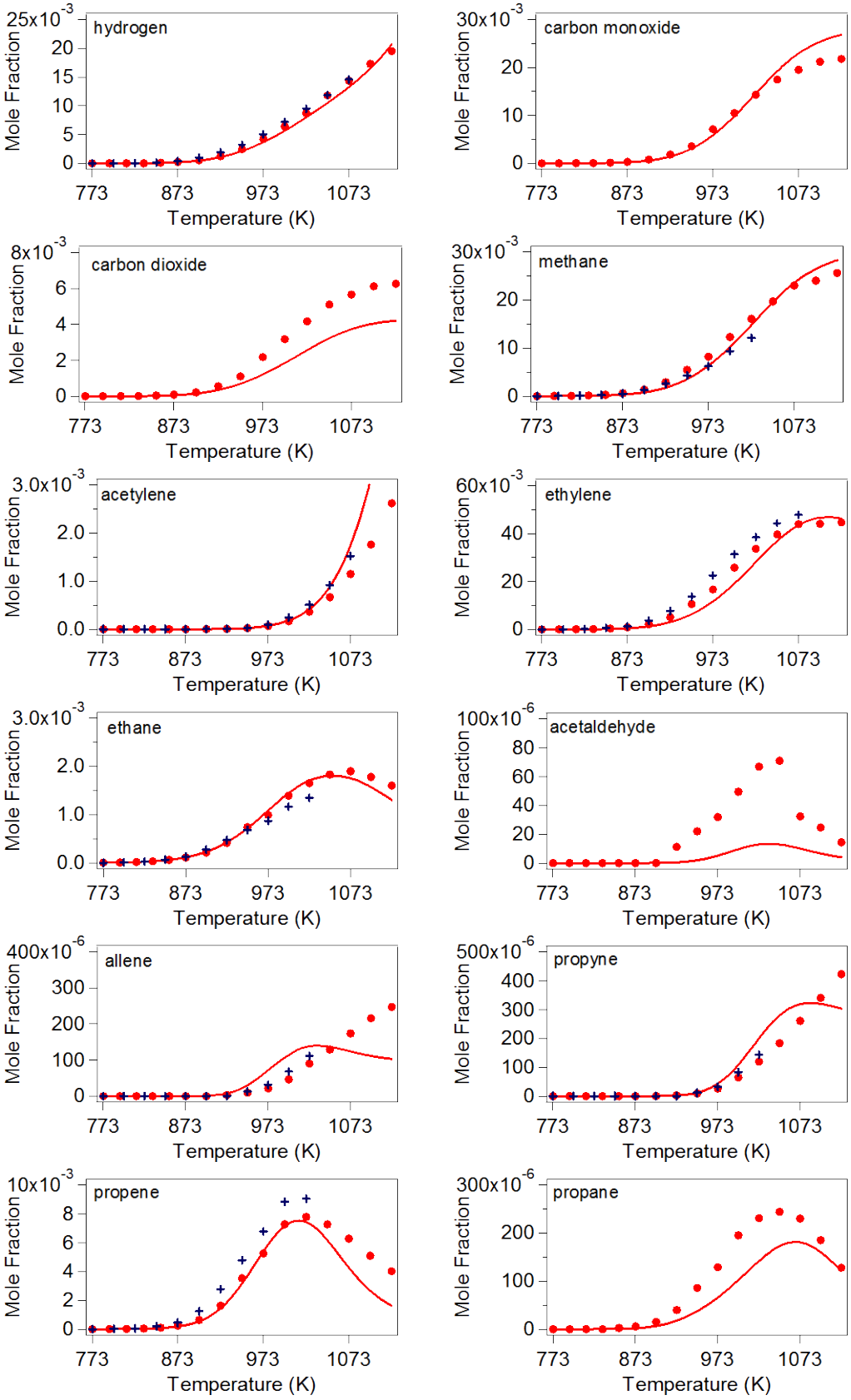

Fig. 4. Evolution of the mole fraction of the reaction products with the temperature at a residence time of 1 s (●: methyl decanoate experiments; +: n-dodecane experiments [25]; line: methyl decanoate simulations). Inlet mole fractions of n-dodecane and methyl decanoate are 0.02 and 0.0218, respectively. Part one.

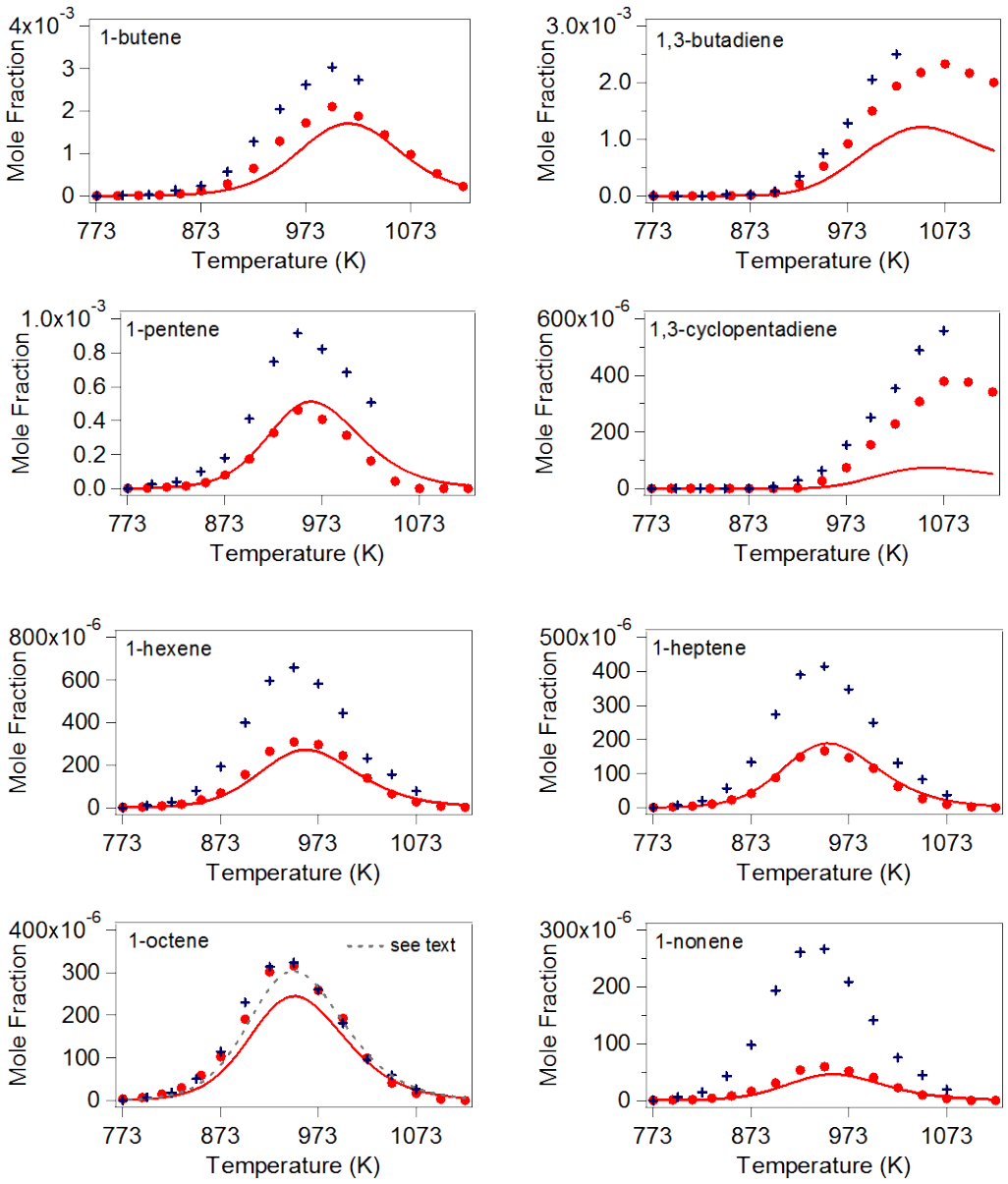

Fig. 5. Evolution of the mole fraction of the reaction products with the temperature at a residence time of 1 s (●: methyl decanoate experiments; +: n-dodecane experiments [25]; line: methyl decanoate simulations). Inlet mole fractions of n-dodecane and methyl decanoate are 0.02 and 0.0218, respectively. Part two.

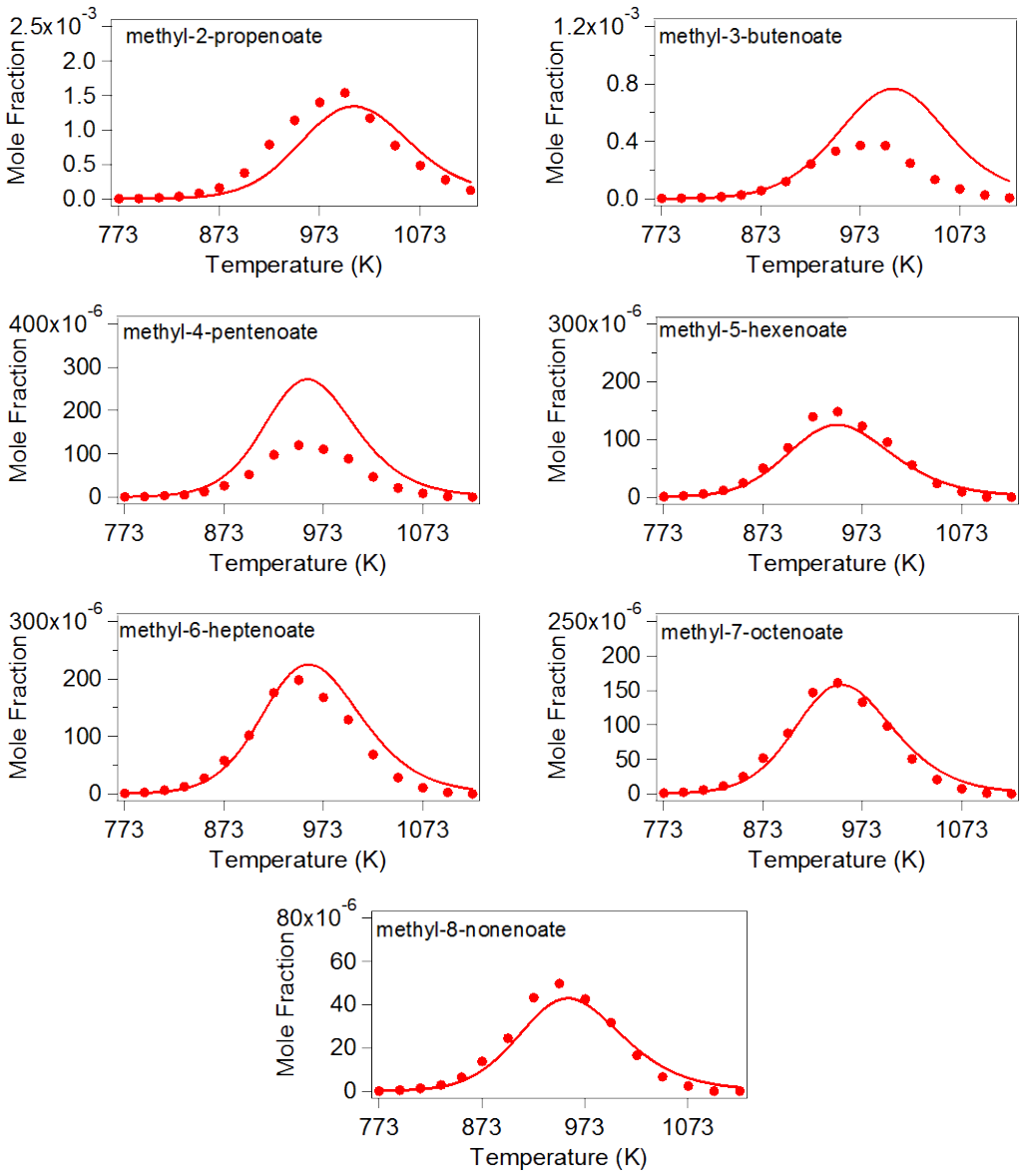

Fig. 6. Evolution of the mole fraction of the reaction products with the temperature at a residence time of 1 s (●: methyl decanoate experiments; line: methyl decanoate simulations). Inlet mole fractions of n-dodecane and methyl decanoate are 0.02 and 0.0218, respectively. Part three.

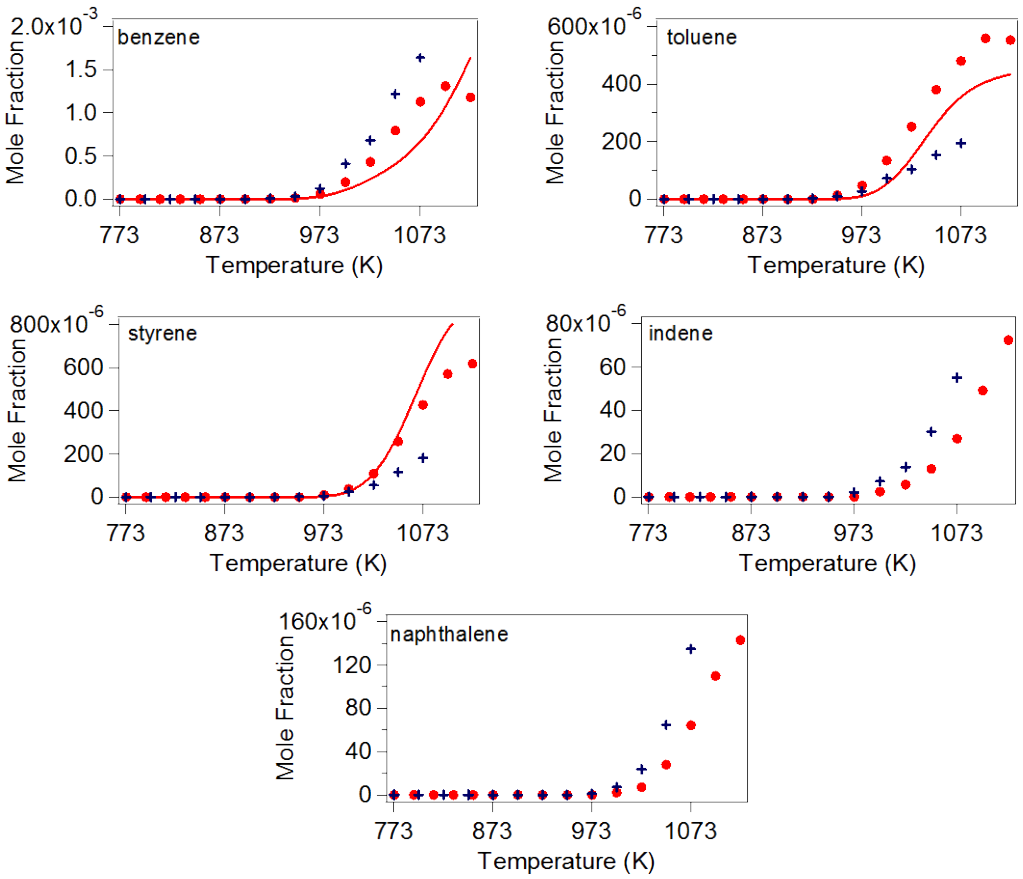

Fig. 7. Evolution of the mole fraction of the reaction products with the temperature at a residence time of 1 s (●: methyl decanoate experiments; +: n-dodecane experiments [25]; line: methyl decanoate simulations). Inlet mole fractions of n-dodecane and methyl decanoate are 0.02 and 0.0218, respectively. Part four.

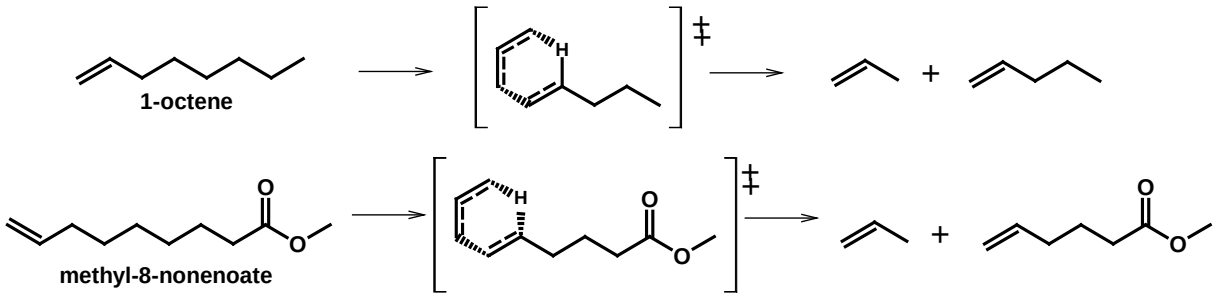

Fig. 8. Retro-ene reactions in the case of 1-octene and methyl-8-nonenoate.

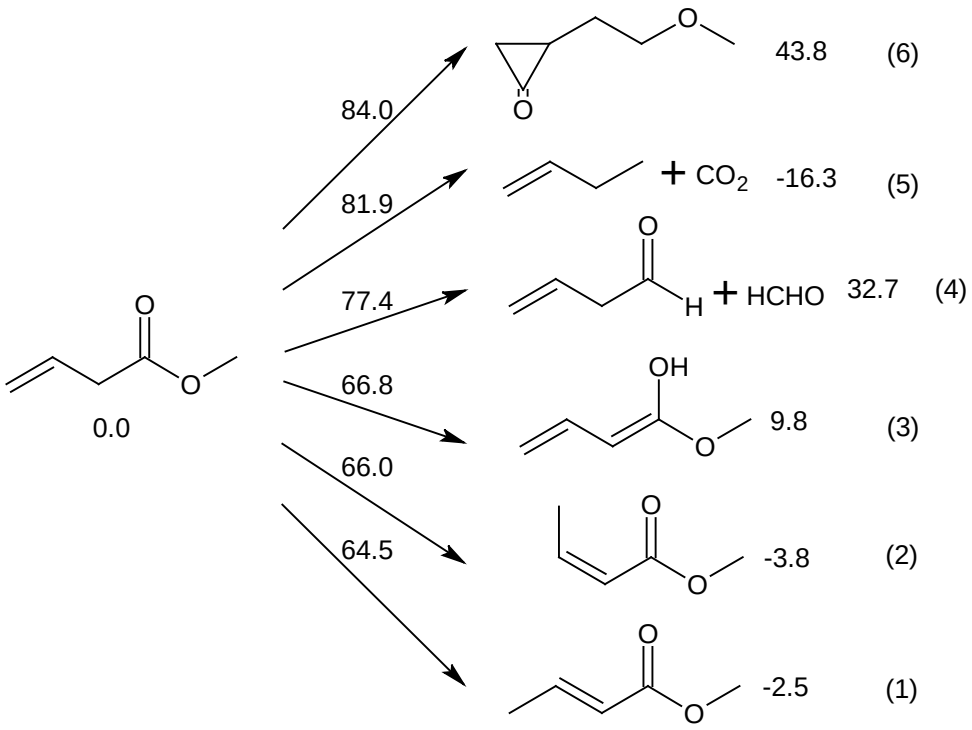

Fig. 9. Molecular reactions of methyl-3-butenoate. Enthalpies of TS and products are calculated at the CBS-QB3 level of theory and are given at 298 K in kcal mol −1 relatively to methyl-3-butenoate.

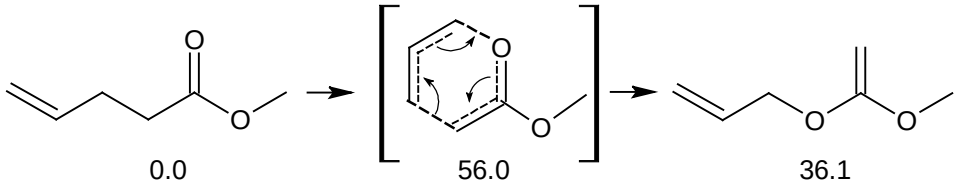

Fig. 10. Molecular reaction of methyl-4-pentenoate. Enthalpies of TS and products are calculated at the CBS-QB3 level of theory and are given at 298 K in kcal mol −1 relatively to methyl-4-pentenoate.

While other alkenes profiles are very well simulated, mole fractions of 1-octene are slightly under-estimated by the model (Fig. 5). 1-octene is mainly formed from the decomposition by β-scission of the $C_{11}H_{21}O_2$ radical (with the same skeleton as the reactant) with the radical center on the fourth carbon atom in the chain (Fig. 11). The activation energy of this reaction is lower than the value used in the case of the breaking of a C-C bond due to the vicinity of the ester group and was calculated theoretically by [12] (Ea = 27,800 cal mol^{-1} instead of 28,700 cal mol^{-1} for other C-C bond breaking in alkyl ester radicals). According to the sensitivity analysis that was performed for 1-octene, the activation energy of the reaction of decomposition by β-scission to 1-octene should be lowered of only 0.5 kcal mol^{-1} so that the model reproduces well the mole fraction profile of 1-octene (dashed line in Fig. 5). This value would be in the uncertainty range of the calculated rate constant and does not change the simulated amounts of other products.

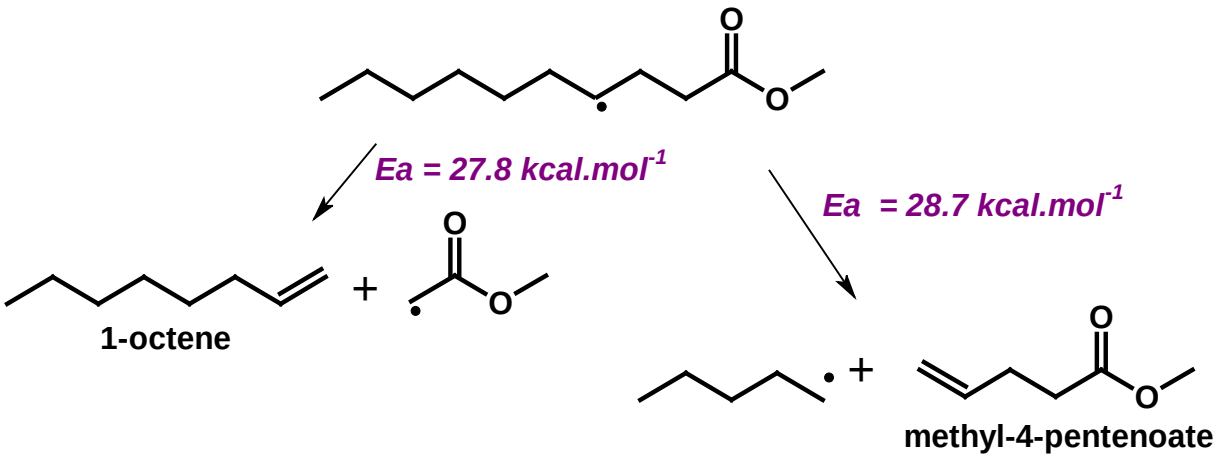

Fig. 11. β-scission decomposition pathways of the $C_{11}H_{21}O_2$ radical (with the same skeleton as the reactant) with the radical center on the fourth carbon atom in the chain.

5.1. Consumption pathways of methyl decanoate

Figure 12 displays the main pathways of consumption of the reactant, methyl decanoate, at a temperature of 900 K and a residence time of 1 s. Under these conditions, the reactant is mainly consumed by H-abstractions by H-atoms, methyl and ethyl radicals. The main radical obtained through these H-abstractions is radical R28 in Fig. 12 with the radical center in position 2 in the alkyl chain (see Fig. 1 for the numbering of carbon atoms in the alkyl chain of methyl decanoate). The dissociation energy of this C-H bond is relatively low (94.3 kcal mol^{-1} whereas it is 98.8 kcal mol^{-1} for a secondary C-H bond [45]). Thus 43.7% of methyl decanoate is consumed to give radical R28. 12.6% of methyl decanoate is consumed to yield radical R27 (H-abstractions of an H-atom of the methyl group in the ester function) and 5.7% to radical R26 (H-abstractions of an H-atom of the other methyl group in the alkyl chain). The seven other possible radicals (from R29 to R35) are obtained through H-abstractions of secondary H-atoms. Each of them represents 5% of the consumption of the reactant.

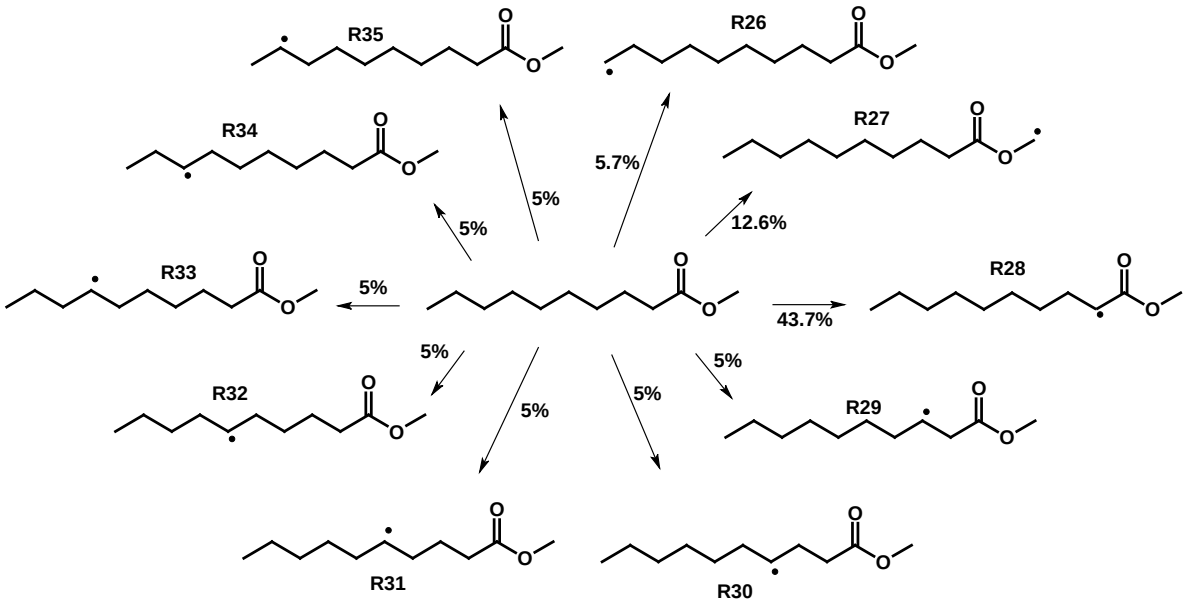

Fig. 12. Main pathways of consumption of methyl decanoate (τ = 1 s, T = 900 K).

5.2. Formation of carbon oxides and acetaldehyde

The use of a methanizer allowed the detection of the presence of small amounts (a few ppm) of carbon oxides at 773 K, the lowest temperature investigated in this study, for which a very low conversion of 0.07% was measured. The CO_2 to CO mole fraction ratio was calculated over the whole range of temperatures. It is around 0.7 at 773 and 793 K. It decreases in an abrupt manner from 0.7 to 0.3 between 793 and 833 K (the conversion increases from 0.17% to 0.81%) and remains around this value at higher temperatures. This means that the formation of carbon dioxide is enhanced at very low conversion and that a change in the reaction pathways is likely occurring in the temperature range 773–793 K. This change could be due to a homogeneous molecular reaction (with a low activation energy) forming directly CO_2 from the reactant or to a heterogeneous reaction at the wall of the reactor. Heterogeneous reactions are more probable than a molecular reaction at 773 K since the latter one should involve a very low activation energy. Brocard and Baronnet studied the pyrolysis of methyl tert-butyl ether in different closed vessels (packed and unpacked, coated and uncoated) [47]. They observed large changes in the reactivity of the system due to important wall effects. These reactions (molecular and heterogeneous) would be also important at higher temperature, but their effect would be masked by the chain radical mechanism occurring at higher temperatures. Note that the sequence of reactions proposed by Dagaut et al. [10] for the early production of carbon dioxide (unimolecular initiation by breaking of the CH_3-O bond followed by the decomposition into CO_2 and an alkyl radical) is included in the model but does not play a significant role. This was expected as this bond has a relatively high dissociation energy (85.7 kcal mol^{-1} [45]).

The CO_2 to CO mole fraction ratio was also calculated from the data computed with the model. The computed values are similar in the range 800–900 K, but the computed profile is slightly different

from the profile obtained from the experimental data: as expected, there is no abrupt decrease of the ratio at low conversion, since the model does not contain reaction forming CO_2 directly from the reactant.

The reaction pathways from methyl decanoate to carbon monoxide and carbon dioxide were investigated from a rate of production analysis at a temperature of 900 K ([Fig. 13] and [Fig. 14]). Percentages given in [Fig. 13] and [Fig. 14] are related to the consumption of the reactant (as an example, 1.13% between R43 and R21 in Fig. 14 means that this reaction corresponds to 1.13% of the consumption of the initial reactant, methyl decanoate). As expected, CO and CO_2 come from the decomposition of the ester group of the molecule in chain propagation reactions. Carbon monoxide is mainly obtained from the decomposition of $C_{11}H_{21}O_2$ radicals with the radical center located in position 4 and 6. These radicals decompose by successive reactions of β-scission leading to a $C_3H_5O_2$ radical (R42 in Fig. 13). The reaction of β-scission leading to the formation of ketene (not shown in Fig. 13) is disfavored by a high activation energy and this radical mainly isomerizes by shifting an H-atom from the methyl group of the ester function to the methylene group. Then the new radical leads to CO through two successive reactions of β-scission.

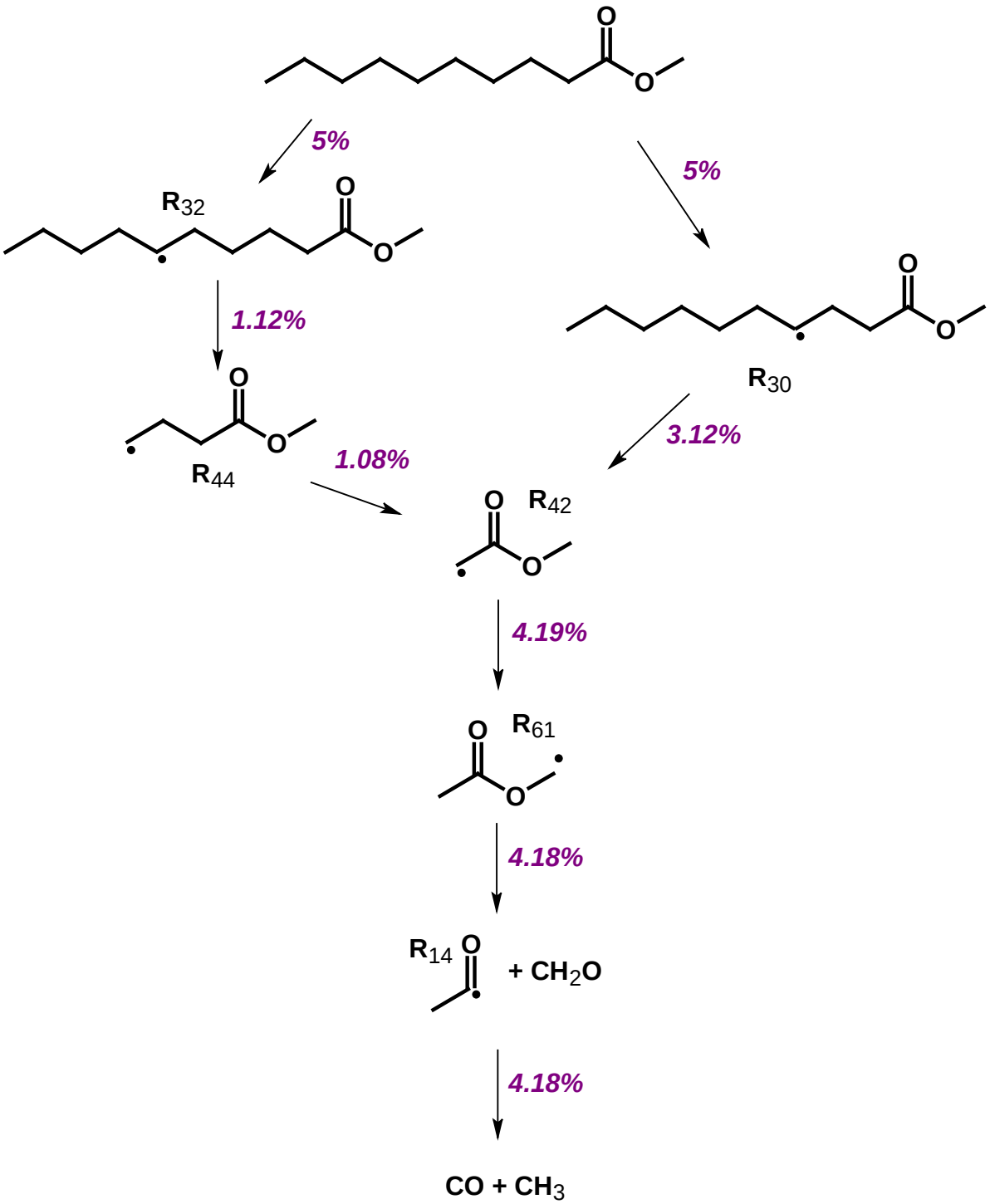

Fig. 13. Route of the formation of carbon monoxide (τ = 1 s, T = 900 K). Percentages are relative to the initial reactant, methyl decanoate.

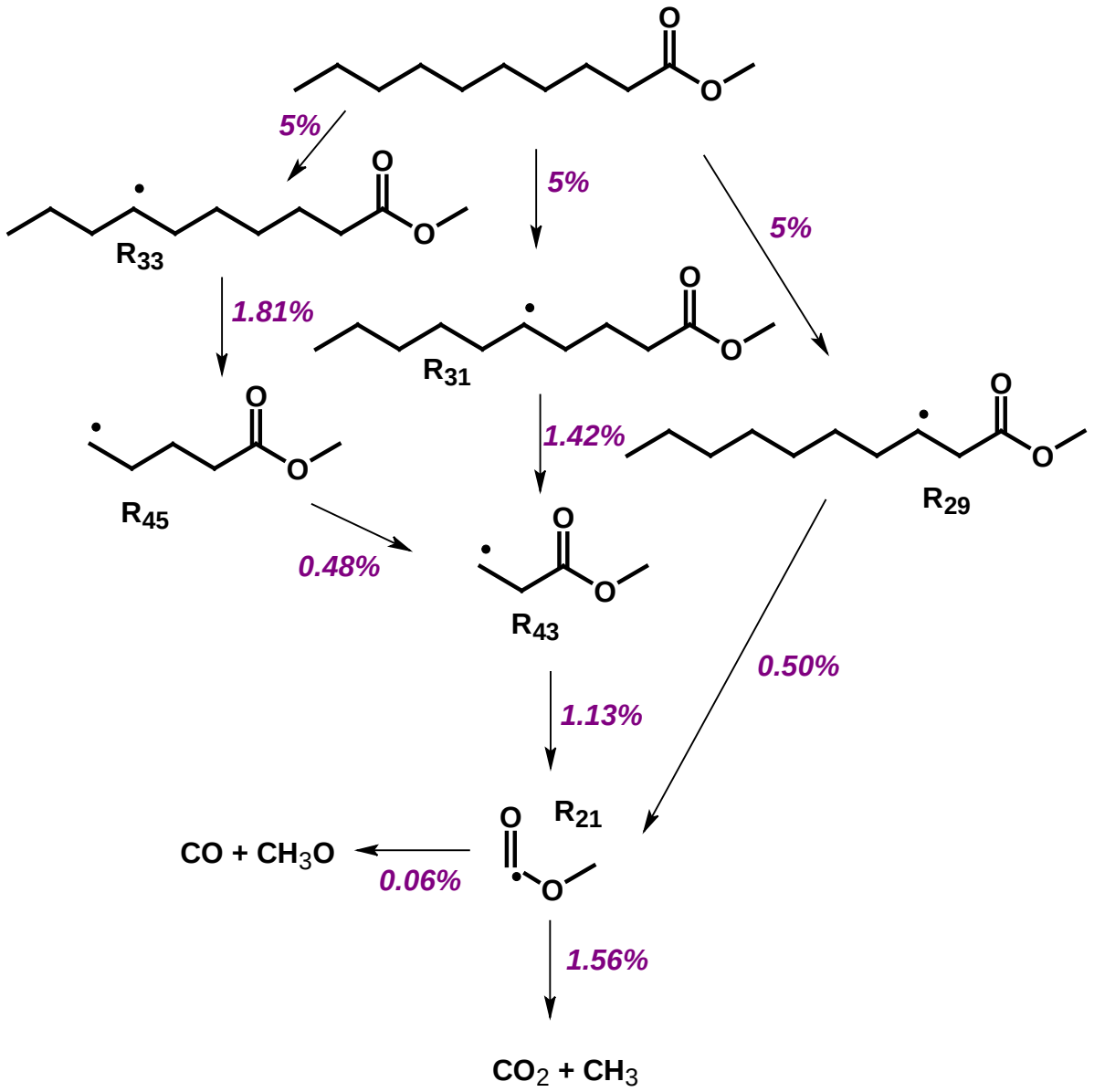

Fig. 14. Route of formation of carbon dioxide (τ = 1s, T = 900 K). Percentages are relative to the initial reactant, methyl decanoate.

The formation of CO_2 (Fig. 14) mainly occurs through the decomposition by β-scission of $C_{11}H_{21}O_2$ radicals with the radical center located in position 3, 5 and 7. Note that the $C_2H_3O_2$ radical (R21 in Fig. 14) which is involved in the successive β-scissions can decompose either into CO_2 or CO but that the decomposition into CO_2 is prevalent (the ratio of both rates is about 26 at 900 K). The $C_{11}H_{21}O_2$ radical with the radical center located in position 2 (the major one which is obtained by H-atom abstraction from the reactant) does not decompose by β-scission as other $C_{11}H_{21}O_2$ radicals R30, R31, R32 and R33 do (see [Fig. 13] and [Fig. 14]). This radical mainly isomerizes to R31 and R32 which then lead to CO and CO_2 as shown in [Fig. 13] and [Fig. 14].

Acetaldehyde is mainly formed from the addition of methyl radicals to formaldehyde, followed by a reaction of decomposition by β-scission. The main source of formaldehyde is the decomposition of the radical R61 in Fig. 13. The under-prediction of the mole fractions of acetaldehyde is likely due to missing pathway in the secondary mechanism (e.g., reactions of consumption of primary oxygenated products).

5.3. Role of retro-ene reactions

The kinetic analysis of the mechanism shows that the retro-ene reactions play a role in the consumption of 1-olefins and esters having one double bond at the extremity of the chain (Fig. 8). At 900 K, the retro-ene reaction is responsible for 60% of the consumption of 1-octene. This type of reaction also plays a role in the formation of propene at temperature higher than 830 K. Below 830 K, propene is mainly formed by the radical mechanism and retro-ene reactions play a minor role. At 1000 K, the retro-ene reactions are responsible for 53% of the formation of propene. At 1100 K, they only represent 27% of its formation.

5.4. Formation of aromatics

The kinetic analysis of the model shows that benzene is formed through two main pathways. The first one is the decomposition of 1,3-cyclohexadiene to benzene + H_2 (69% of the formation of benzene at 900 K) and the second one is the recombination of two propargyl radicals, C_3H_3 (30% of the formation of benzene at 900 K). Propargyl radicals come from the H-atom abstractions on allene and propyne (C_3H_4) and 1,3-cyclohexadiene comes from the reaction of C_2H_3 radicals to 1,3-butadiene. Benzene is mainly consumed by H-atom abstractions by H-atoms, CH_3 and C_2H_5 radicals to form phenyl radicals. Benzene also reacts through ipso-addition with C_2H_3 radicals to form styrene + H. Phenyl radicals recombine with methyl radical to form toluene and add to ethylene to form C_8H_9 radicals that easily decompose to styrene + H. Toluene is also formed from benzyl radicals (through H-atom abstractions) which comes from the reaction of cyclopentadienyl radicals (C_5H_5) with ethylene.

Toluene is fairly well reproduced by the model, meaning that the concentrations of the phenyl and methyl radicals are likely well predicted. The correct prediction of the concentration of the methyl radical by the model is also confirmed by the good agreement which is observed for species such as methane, ethane and propane, which are produced by H-abstraction on the reactant, and combination of two methyl radicals and methyl and ethyl radicals, respectively.

6. Conclusion

In this study, new experimental results of the thermal decomposition of methyl decanoate were obtained in a jet-stirred reactor operated at constant temperature and pressure. Thirty-two reaction products were detected: they were mainly 1-olefins from ethylene to 1-nonene and methyl esters with one double bond at the end of the chain from methyl-2-propenoate to methyl-8-nonenoate. The formation of carbon oxides and acetaldehyde was also observed because of the presence of oxygen atoms in the reactant. The evolution of the ratio of mole fractions of CO and CO_2 with the temperature showed that there is a change in the formation pathways of CO_2 occurring at low conversion.

These new results were compared with previous ones about the pyrolysis of n-dodecane, a linear alkane of similar size. This comparative study showed that both molecules have about the same reactivity, methyl decanoate being slightly more stable than n-dodecane. As far as products are concerned, the main difference is the formation of specific species due to the presence of the ester function in methyl decanoate: unsaturated methyl esters and oxygenated compounds. Mole fractions of olefins are generally lower in the case of methyl decanoate than in the case of n-dodecane due to the competition between the formation of olefins and unsaturated esters from ester-alkyl radicals from methyl decanoate.

A model for the thermal decomposition of methyl decanoate was generated using the software EXGAS. The model reproduces fairly well the conversion of the reactant and the mole fractions of the reaction products. The kinetic analysis showed that retro-ene reactions play an important role in the consumption of olefins and esters with one double bond at the extremity of the chain. The model does not account for the evolution of the CO/CO_2 ratio at low conversion and for the consumption of small unsaturated methyl esters. This is likely due to missing consumption pathways such as molecular reactions. Further investigations are needed to well understand the chemistry involved in the pyrolysis chemistry of methyl esters.

Acknowledgment

This work was funded by the European Commission through the “Clean ICE” Advanced Research Grant of the European Research Council.

References

[1] M.P. Musculus, J.E. Dec, D.R. Tree, SAE Technical Paper Series, 2002-01-0889.

[2] K. Bozbas, Renew. Sust. Energy Rev. 12 (2) (2008), pp. 542–552.

[3] A. Demirbas, Prog. Energy Combust. Sci. 31 (2005), pp. 466–487.

[4] M.S. Graboski and R.L. McCormick, Prog. Energy Combust. Sci. 24 (1998), pp. 125–164.

[5] A.K. Agarwal, Prog. Energy Combust. Sci. 33 (2007), pp. 233–271.

[6] K. Kohse-Höinghaus, P. Oßwald, T.A. Cool, T. Kasper, N. Hansen, F. Qi, C.K. Westbrook and P.R. Westmoreland, Angew. Chem. Int. Ed. 49 (21) (2010), pp. 3572–3597.

[7] S. Bax, M.H. Hakka, P.A. Glaude, O. Herbinet and F. Battin-Leclerc, Combust. Flame 157 (6) (2010), pp. 1220-1229.

[8] M.H. Hakka, P.A. Glaude, O. Herbinet and F. Battin-Leclerc, Combust. Flame 156 (2009), pp. 2129–2144.

[9] T. Vaughn, M. Hammill, M. Harris, A.J. Marchese, Ignition Delay of Bio-Ester Fuel Droplets, SAE Technical Paper Series, 2006-01-3302.

[10] P. Dagaut, S. Gaïl and M. Sahasrabudhe, Proc. Combust. Inst. 31 (2) (2007), pp. 2955–2961.

[11] J.P. Szybist, A.L. Boehman, D.C. Haworth and H. Koga, Combust. Flame 149 (1–2) (2007), pp. 112–128.

[12] P.A. Glaude, O. Herbinet, S. Bax, J. Biet, V. Warth and F. Battin-Leclerc, Combust. Flame 157 (11) (2010), pp. 2035–2050.

[13] O. Herbinet, W.J. Pitz and C.K. Westbrook, Combust. Flame 154 (3) (2008), pp. 507–528.

[14] O. Herbinet, W.J. Pitz and C.K. Westbrook, Combust. Flame 157 (2010), pp. 893–908.

[15] C.D. Hurd and F.H. Blunck, J. Am. Chem. Soc. 60 (10) (1938), pp. 2419–2425.

[16] R.T. Arnold, G.G. Smith and R.M. Dodson, J. Org. Chem. 15 (6) (1950), pp. 1256–1260.

[17] A.T. Blades, Can. J. Chem. 32 (1954), pp. 366–372.

[18] D. Archambault and F. Billaud, Ind. Crop. Prod. 7 (1998), pp. 329–334.

[19] W. Seames, Y. Luo, I. Ahmed, T. Aulich, A. Kubátová, J. Šťávová and E. Kozliak, Biomass Bioenergy 34 (7) (2010), pp. 939–946.

[20] A. Farooq, D.F. Davidson, R.K. Hanson, L.K. Huynh and A. Violi, Proc. Combust. Inst. 32 (1) (2009), pp. 247–253.

[21] E.M. Fisher, W.J. Pitz, H.J. Curran and C.K. Westbrook, Proc. Combust. Inst. 28 (2000) (1579), p. 1586.

[22] W.K. Metcalfe, S. Dooley, H.J. Curran, J.M. Simmie, A. El-Nahas and M.V. Navarro, J. Phys. Chem. 111 (2007), pp. 4001–4014.

[23] S. Gaïl, M.J. Thomson, S.M. Sarathy, S.A. Syed, P. Dagaut, P. Diévart, A.J. Marchese and F.L. Dryer, Proc. Combust. Inst. 31 (2006), pp. 3005–3011.

[24] L.K. Huynh and A. Violi, J. Org. Chem. 73 (2008), pp. 94–101.

[25] O. Herbinet, P.M. Marquaire, F. Battin-Leclerc and R. Fournet, J. Anal. Appl. Pyrol. 78 (2007), pp. 419–429.

[26] V. Warth, N. Stef, P.A. Glaude, F. Battin-Leclerc, G. Scacchi and G.M. Côme, Combust. Flame 114 (1998), pp. 81–102.

[27] F. Buda, R. Bounaceur, V. Warth, P.A. Glaude, R. Fournet and F. Battin-Leclerc, Combust. Flame 142 (2005), pp. 170–186.

[28] J. Biet, M.H. Hakka, V. Warth, P.A. Glaude and F. Battin-Leclerc, Energy Fuel 22 (2008), pp. 2258–2269.

[29] J.L. Houzelot and J. Villermaux, Chem. Eng. Sci. 32 (12) (1977), pp. 1465–1470.

[30] J.L. Houzelot and J. Villermaux, Chem. Eng. Sci. 39 (9) (1984), pp. 1409–1413.

[31] R. David and D. Matras, Can. J. Chem. Eng. 53 (1975), p. 297.

[32] H.A. Gueniche, P.A. Glaude, R. Fournet and F. Battin-Leclerc, Combust. Flame 151 (1–2) (2007), pp. 245–261.

[33] P. Barbé, F. Battin-Leclerc and G.M. Côme, J. Chim. Phys. 92 (1995), pp. 1666–1692.

[34] I. Da Costa, R. Fournet, F. Billaud and F. Battin-Leclerc, Int. J. Chem. Kinet. 35 (2003), pp. 503–524.

[35] R. Bounaceur, I. Da Costa, R. Fournet, F. Billaud and F. Battin-Leclerc, Int. J. Chem. Kinet. 37 (2005), pp. 25–49.

[36] W. Tsang, Int. J. Chem. Kinet. 10 (1978), pp. 1119–1138.

[37] C. Richard, G. Scacchi and M.H. Back, Int. J. Chem. Kinet. 10 (1978), pp. 307–324.

[38] M.J. Frisch et al., Gaussian03, Revision B05; Gaussian, Inc., Wallingford, CT, 2004.

[39] J.A. Montgomery, M.J. Frisch, J.W. Ochterski and G.A. Petersson, J. Chem. Phys. 110 (1999), pp. 2822–2827.

[40] V. Mokrushin, W. Tsang, Chemrate v.1.5.2; NIST, Ed. Gaithersburg, MD 20899, USA, 2006.

[41] H.S. Johnston and J. Heicklen, J. Phys. Chem. 66 (1962), pp. 532–533.

[42] C. Muller, V. Michel, G. Scacchi and G.M. Côme, J. Chim. Phys. 92 (1995), pp. 1154–1177.

[43] S.W. Benson, Thermochemical Kinetics (second ed.), Wiley, New York (1976).

[44] R.J. Kee, F.M. Rupley, J.A. Miller, Chemkin II: A FORTRAN Chemical Kinetics Package for the Analysis of a Gas-phase Chemical Kinetics, SAND89-8009B, Sandia Laboratories, 1993.

[45] A.M. El-Nahas, M.V. Navarro, J.M. Simmie, J.W. Bozzelli, H.J. Curran, S. Dooley and W. Metcalfe, J. Phys. Chem. A 111 (19) (2007), pp. 3727–3739.

[46] M.H. Hakka, H. Bennadji, J. Biet, M. Yahyaoui, V. Warth, L. Coniglio, O. Herbinet, P.A. Glaude, F. Billaud and F. Battin-Leclerc, Int. J. Chem. Kinet. 42 (2010), pp. 226–252.

[47] J.C. Brocard and F. Baronnet, J. Chim. Phys. 84 (1987), pp. 19–25.